**Use Authorization**

In presenting this thesis partially fulfilling the requirements for an advanced degree at Idaho State University, I agree that the library shall make it freely available for inspection. I further state that permission for extensive copying of my thesis for scholarly purposes may be granted by the Dean of Graduate School, the Dean of my academic division, or the University Librarian. It is understood that any copying or publication of this thesis for financial gain shall not be allowed without my written permission.

Signature ___________________________________

Date________________________________________

# Study on the effect of dielectric constant in the RSSI-based RFID indoor localization using supervised machine learning algorithms.

by

Suman Neupane

A thesis

submitted in partial fulfillment

of the requirements for the degree of

Master of Science in the Department of Electrical and Computer Engineering

Idaho State University

Summer 2023

## Committee Approval

To the Graduate Faculty:

The committee members appointed to examine the thesis of Suman Neupane find it satisfactory and recommended that it be accepted.

**Dr. Andrew Chrysler**

Major Advisor

**Dr. Mostafa Fouda**

Committee Member

**Dr. Mustafa Mashal**

Graduate Faculty Representative

## Acknowledgments

I would like to thank everyone who helped me persevere through this research in a direct and indirect manner. It would not have been possible to complete this research with the unwavering support I received from my advisor, family, and friends. I would like to start by expressing my sincere gratitude to my advisor, Dr. Andrew Chrysler, for his immense support and erudite guidelines which helped me complete my thesis. I would also like to thank Dr. Mostafa Fouda, the committee member, and Dr. Mustafa Mashal, the graduate faculty representative for this thesis. I would like to thank the entire department of Electrical and computer engineering department and graduate school at Idaho State University for their support in making this research successful.

**Table of Contents**

**List of Figures**

## List of Tables

Study on the effect of dielectric constant in the RSSI-based RFID indoor localization using supervised machine learning algorithms.

Thesis Abstract - Idaho State University (2022)

Passive RFID tags are widely used for indoor localization. However, a variety of environmental factors tend to reduce the localization accuracy. This research explores how different relative dielectric constants impact RSSI-based RFID Indoor localization. Three ML algorithms (1) k-NN, (2) XGBoost, and (3) Decision Tree are used for the indoor localization of Cantaloupe, Cabbage, and Pineapple which have different dielectric values. XGBoost achieved an accuracy of 54.3% for cantaloupe which has a low dielectric value. For pineapple and cabbage which has relatively close dielectric value, the same algorithm achieved comparable accuracy of 76.9% and 78.34% respectively. This research demonstrates the importance of the object's dielectric constant when developing RSSI-based indoor localization systems.

Keywords—dielectric constant, Ultra High Frequency (UHF), Radio Frequency Identification (RFID) tags, ML algorithm, indoor localization.

# CHAPTER 1. INTRODUCTION

## 1.1 Background and Motivation

Indoor localization is the method of obtaining the location of a user or device in the indoor environment. Global positioning system (GPS) is used worldwide for outdoor localization, but it cannot detect objects located inside the building. Hence there is a requisite of detecting and locating objects or user in the indoor setting, especially in the sectors such as agriculture, robotics, supply chain management, and more [1]. Radio Frequency Identification (RFID) utilizes radio waves that enable us to identify, track, and locate items equipped with RFID tags [2]. While the roots of RFID technology can be traced back to World War II [3], Mario W. Cardullo first received the U.S. patent for an active RFID tag with rewritable memory in 1973 [4]. Figure 1.1 shows the first chip installed in a fighter plane near the end of World War II in 1944.

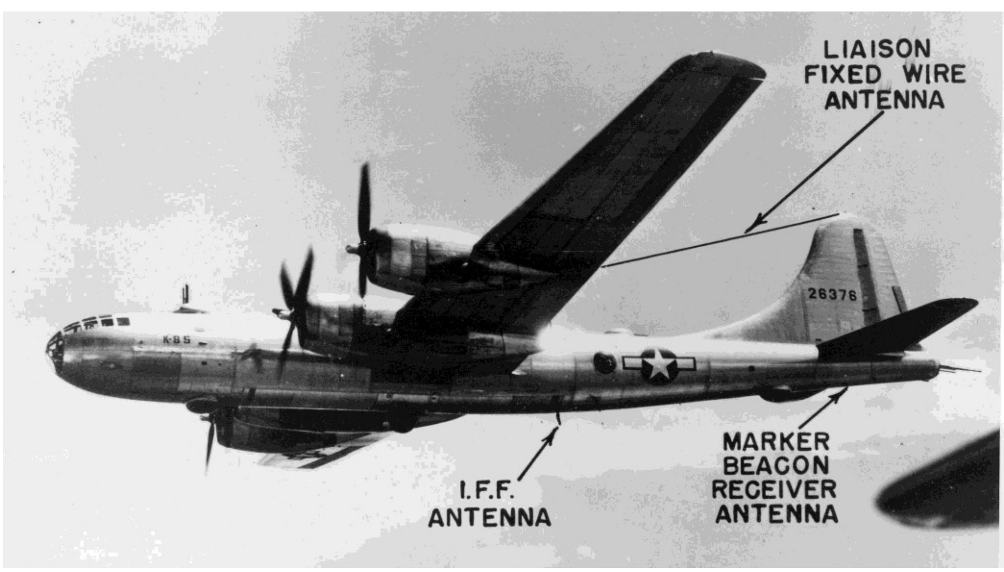


Figure 1.1: Portside antennas on Boeing yb-40 flying fortress [3].

Based on the frequency of operation RFID system are classified into Low Frequency (LF) [120-145 kHz], High Frequency (HF) [13-56 MHz], Ultra High Frequency (UHF) [850-950 MHz], and Super High Frequency (SHF) [2.45-5.8 GHz] [5]-[6]-[7]. SHF band is used for microwave application and resonant frequency are designed to be operated at 2.45 GHz and 5.8 GHz. Further RFID tags can be classified into three major types: active, semiactive, and passive tags [8]. While active and semiactive RFID tags have on-board power supply, passive RFID tag do not possess an on-board power supply and rely only on the power emitted from the reader for both data processing and transmission. A basic RFID system consists of a reader, tags, antenna, and a data collecting device as shown in Figure1.2 [9].

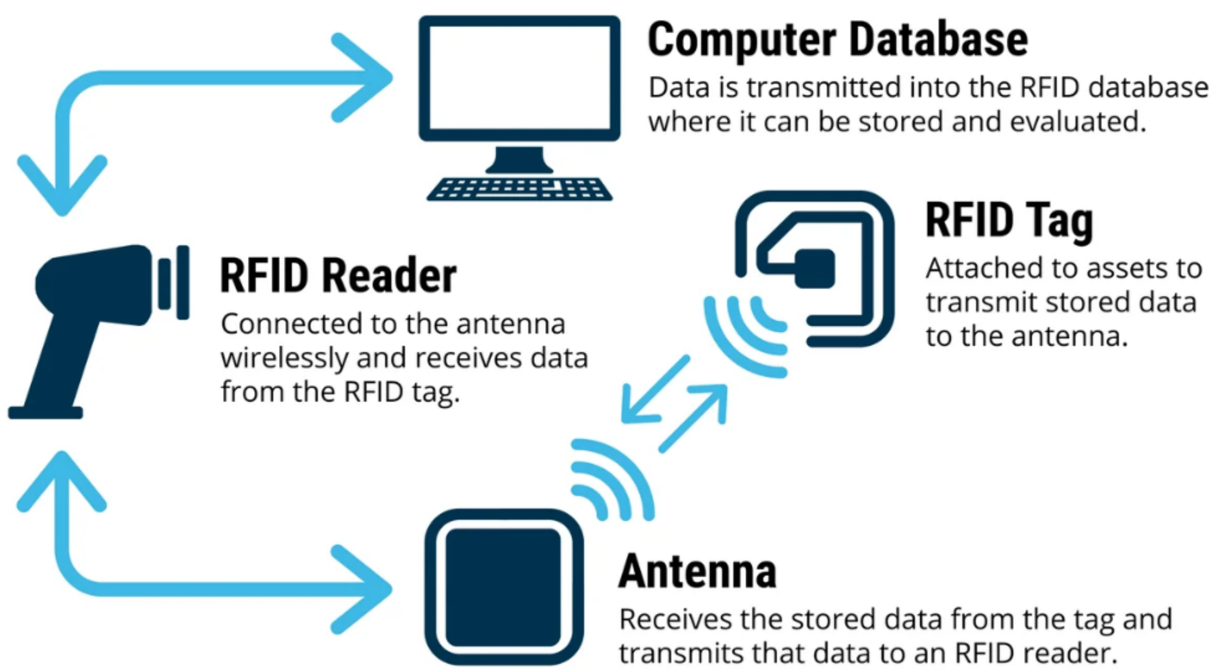


Figure 1.2: Components of Basic RFID System [9].

Artificial Intelligence (AI) is the method of performing human-like intelligence like decision making, learning, and results analysis by intelligent machines [10]. AI enables machines to perform feats of human-like intelligence by making them learn from available resources such as big data and Machine Learning (ML) algorithms. Big data availability and higher computing power has enabled AI to be more efficient which is expected to transform different sectors like transportation [11], engineering [12], health care [13], agriculture [14], job market [15] and more. Development of AI and ML algorithms can be implemented to build robust and more precise RFID indoor localization system.

## 1.2 Problem Statement and Scope

Research on RFID applications is increasing every year with 4% of research being focused on indoor localization system as shown in Figure 1.3 [16]. RFID tags have been used in the tracking and management in different applications like circulation and tracking of books in libraries [17], tracking and managing medications and patients in hospitals [18], verifying authentication of halal foods [19], and more. Many commercial RFID tags are designed for placement on high dielectric objects and thus there is a limited effect when reading a tag's electronic product code (EPC) - even on many high dielectric objects. The issue arises once we try to localize different products/items based on the EPCs of RFID tags equipped on them, where not only the EPC values are significant, but additional information such as received signal strength indicator (RSSI) and phase are required to perform computations/analysis to find localized coordinates. This often results in lower localization accuracy in RFID systems [20]. Research involving RFID indoor localization typically does not consider the electromagnetic properties of the object being equipped with RFID tags for localization.

In this research, we explore the effect of dielectric constant on object localization with UHF RFID tags and give an insight into the impact of dielectric constants on RSSI-based indoor localization utilizing supervised ML algorithms. This novel work considers the material properties of products/items equipped with RFID tags for the purpose of indoor localization.

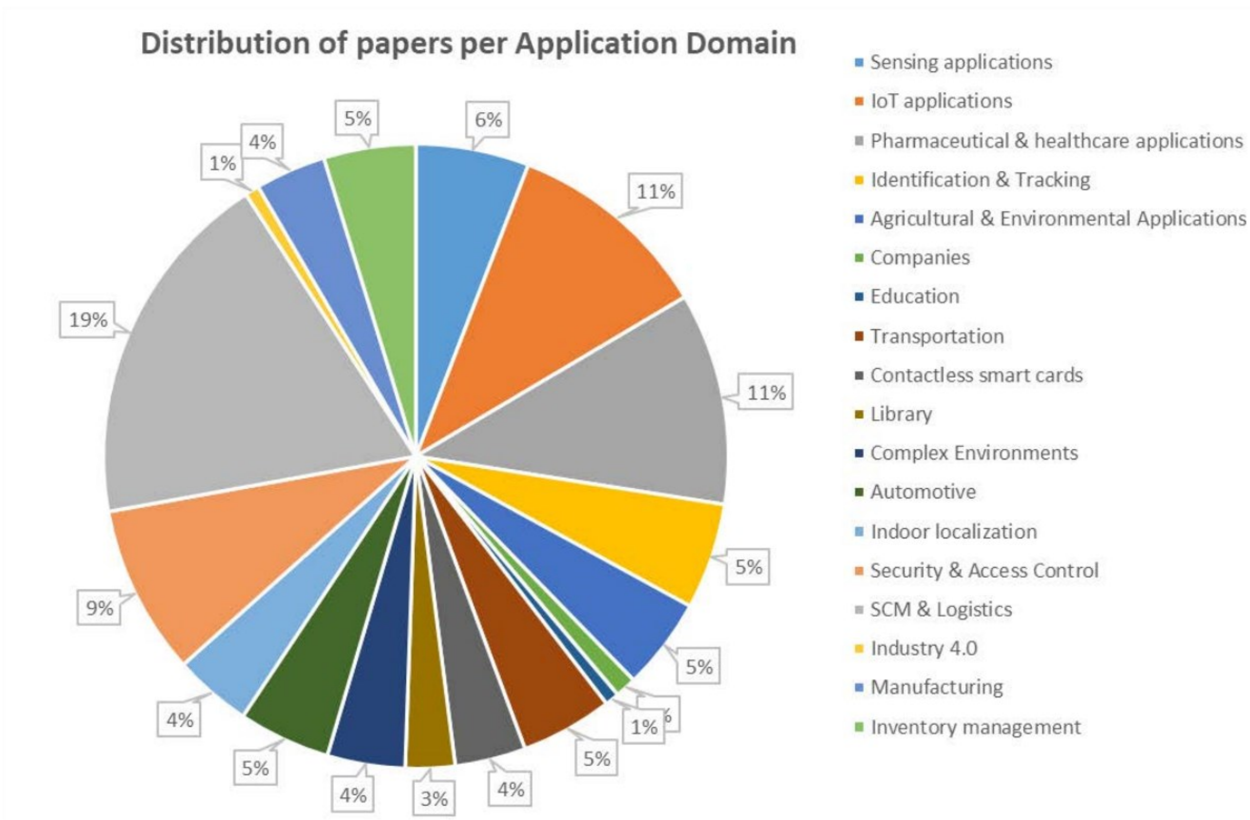


Figure 1.3: Application domain research in RFID [16].

### 1.3 Research Objectives

Following are the research objectives:

1. Explore and study the effect of dielectric constant on object localization with UHF RFID tags.

2. Provide an insight into the impact of dielectric constant on RSSI-based indoor localization.
3. Evaluate the utilization of RFID data in fusion with state-of-the-art ML algorithms.
4. Give future directions into building more precise indoor localization systems utilizing RFID systems by considering object's properties.

## 1.4 Thesis structure

Figure 1.4 shows the thesis structure.

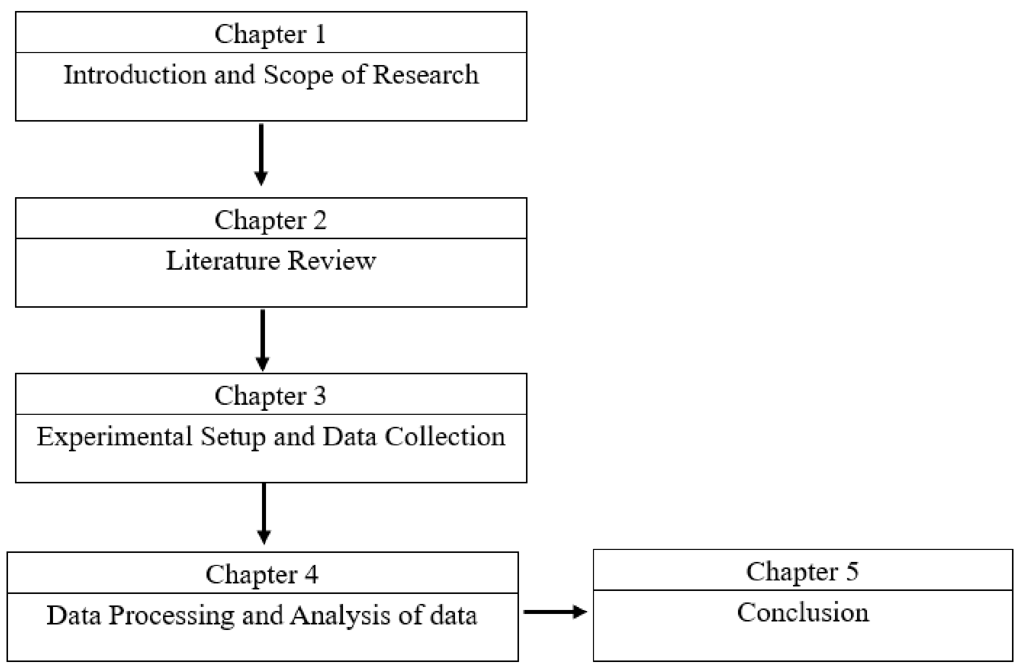


Figure 1.4: Thesis structure

## 1.5 Thesis overview

Chapter 1 provides a brief overview of the introduction of RFID systems and ML algorithms along with scope and current research trend involving RFID. Chapter 2 delves into the literature review of RFID indoor localization, ML algorithms, and dielectric of foods. Chapter 3 provides the details on experimental setup and data collection process. Details of different equipment and software utilized are also described in chapter 3. Chapter 4 delves into data analysis, performance of different supervised algorithms utilized in the data analysis process followed by conclusion in chapter 5.

# CHAPTER 2. LITERATURE REVIEW

## 2.1 Overview of different machine learning algorithms

ML is seen as a subset of AI that performs specific task based on scientific study of algorithms and statistical methods [21]. The most commonly utilized ML methods are supervised learning, unsupervised learning, semi-supervised learning, and reinforcement learning [22]. Less commonly used ML algorithms include batch learning, online learning, instance-based learning, model-based learning, multi-task learning, and transductive learning [23]. The relation between AI, ML, and commonly used ML algorithms is shown in Figure 2.1.

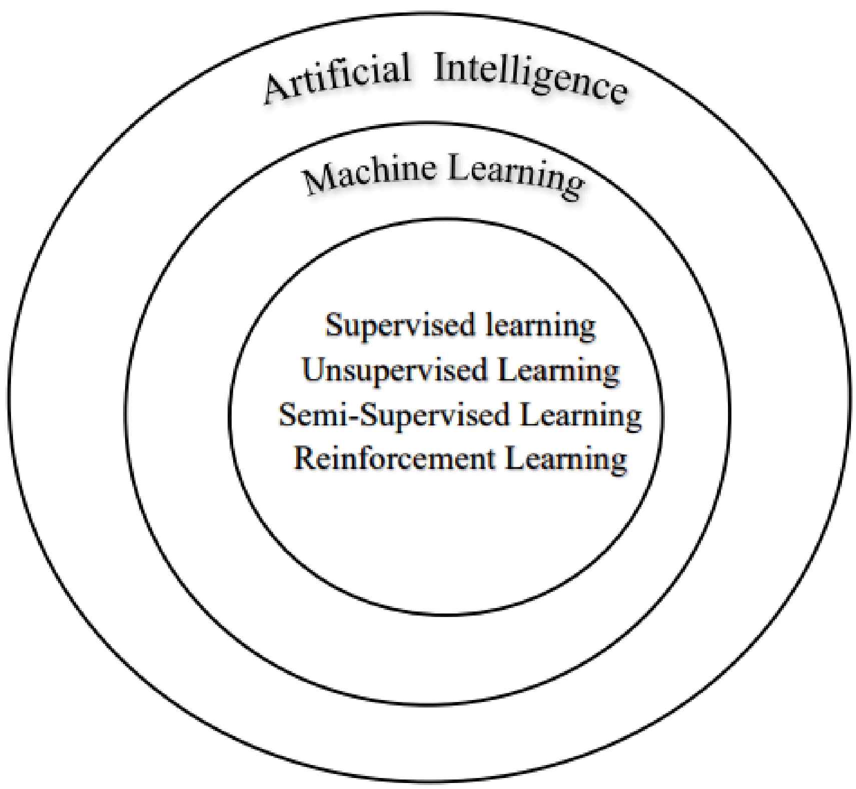


Figure 2.1: Relation between AI, ML, and commonly used ML algorithms

### 2.1.1 Supervised Learning

In supervised learning, the training data with desired solutions (labels) is fed into the algorithm [24]. After training, the algorithm will be able to give predictions to all possible inputs. Some of the most commonly used supervised algorithms include k-Nearest Neighbors (k-NN), Linear Regression, Logistic Regression, Support Vector Machines (SVMs), Decision Trees, Random Forests, Deep Learning (DL), and Neural networks [24].

### 2.1.2 Unsupervised Learning

In unsupervised learning, the training data is unlabeled so the expected result is unknown [24]. After training and learning, the algorithm gives a structure for data after identification of similar data type. Some of the most commonly used unsupervised algorithms include K-means clustering, DBSCAN, Principal Component Analysis (PCA), and t-distributed stochastic neighbor embedding (t-SNE) [24].

### 2.1.3 Semi-supervised Learning

Semi-supervised Learning involves training with partially labeled training data with most of the data being unlabeled and little bit of labeled data. Most semi-supervised algorithms are results of combinations of supervised and unsupervised algorithms [24].

### 2.1.4 Reinforcement Learning

Reinforcement learning (RL) involves a learning system where an agent interacts with the environment and performs certain tasks and gets rewards or penalties. The agent then learns to find the best strategy (policy) to get utmost rewards [24]. An example of reinforcement learning is DeepMind's AlphaGo program [24].

## 2.2 Overview of RFID System

An RFID system no matter the frequency of operation subsist of elements: RFID tags, RFID readers, and middleware (a software interface) [25].

### 2.2.1 RFID Tags

An RFID tag or transponder is an electronic identification support which is often composed of an electronic circuit (for storing information) and an antenna (for receiving waves) [26]. Recent years has seen an increasing amount of research in RIFD chipless technology to mitigate the high cost and low deployment of RFID system [27]-[28]. In chipless RFID, the tag is equipped with a planar encoder and sometimes an antenna to communicate with the reader or interrogator [28]. Figure 2.2 [29] and Figure 2.3 [30] show the chipped RFID tag and chipless RFID tag design respectively. The maximum distance at which an RFID reader can detect the backscattered signal from the tag is the read range and it varies from ranges as far as 12 meters for passive RFID tag whreas active tags can achieve ranges of 100 meters or more [31].

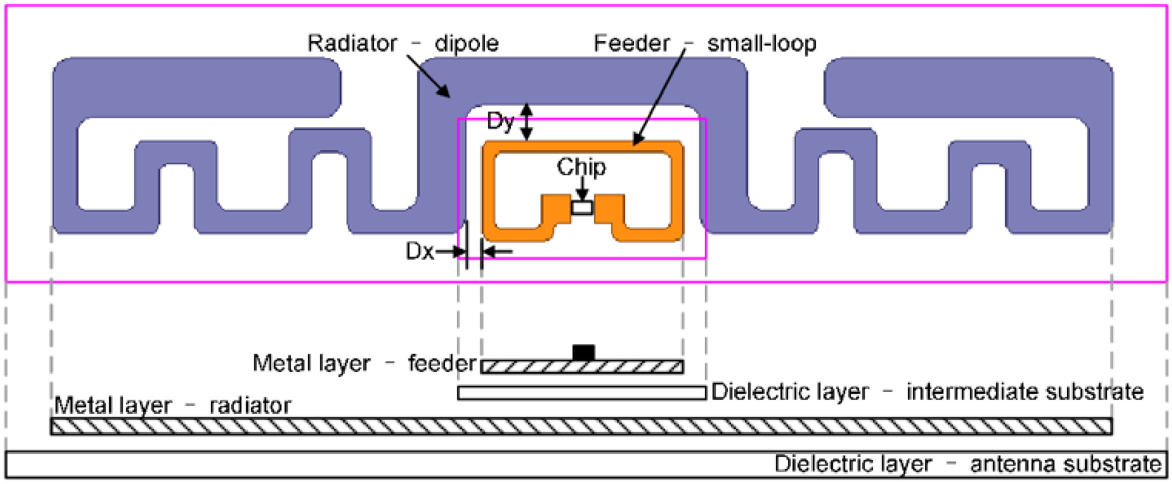


Figure 2.2: Multilayer RFID tag antenna design [29].

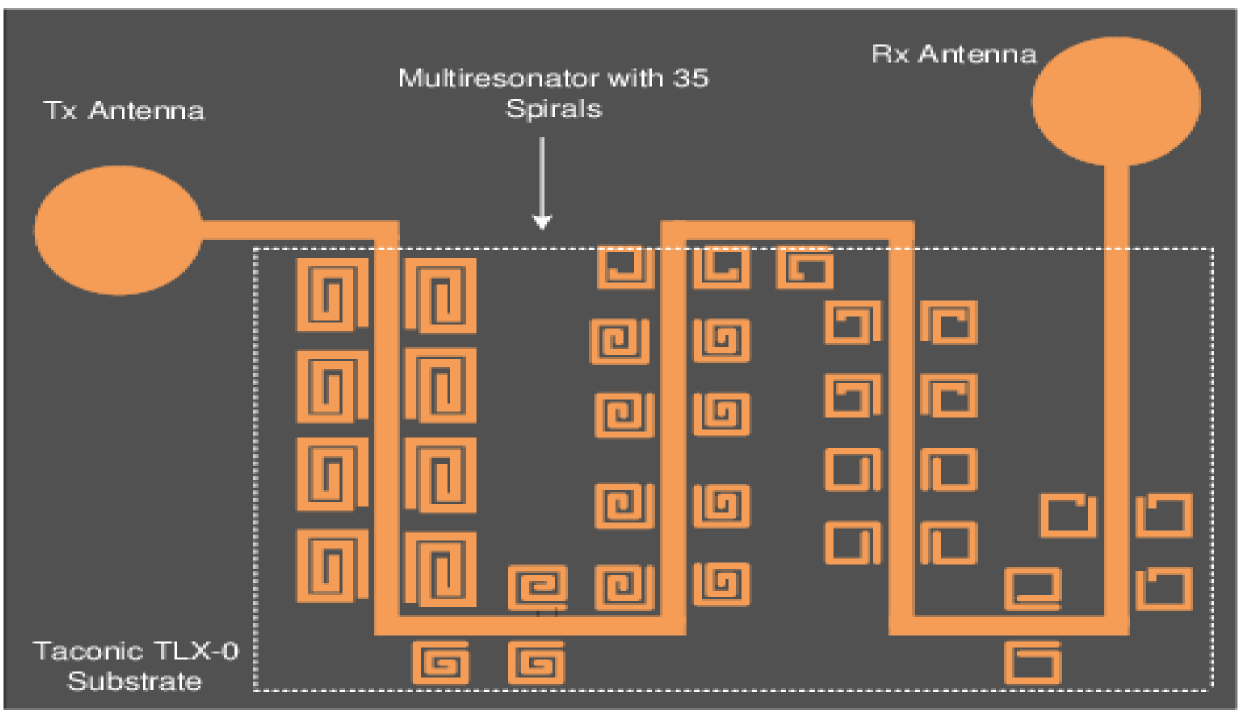


Figure 2.3: 35-bit chipless RFID tag design [30].

### 2.2.2 RFID reader

As the name suggests, RFID reader is a electromagnetic device, equivalent to scanner, which interrogates the data stored in RFID tag [32]. RFID readers can be handheld or fixed and can read multiple tags simultaneously even in non-line-of-sight and embedded inside packaging which does so by transmitting and receiving radio waves using connected antennas [33]. The information read by the reader is then sent to middleware for processing.

### 2.2.3 RFID Middleware

RFID Middleware is a set of software applications that manages the process the vast amount of data collected from the RFID tags and RFID reader [34]. RFID middleware ensures the interface between data collected and information system for both software and hardware of RFID system [35]. It is especially integral to information technology based on Extensible Markup Language (XML), Simple Object Access Protocol (SOAP), Web services, SOA, Web 2.0 infrastructure, and Lightweight Directory Access Protocol (LDAP) [36]-[37].

## 2.3 Related work on RFID Indoor Localization

Different types of techniques like triangulation, multilateration, Bayesian inference, nearest-neighbor (NN), kernel-based learning, and proximity have been utilized in indoor localization [38]-[39]. RFID indoor positioning techniques utilized currently can be classified into one-dimensional, two-dimensional, and three-dimensional positioning. Among which three-dimensional positioning has gained much popularity because of its expected application in different sectors.

In a one-dimensional location system, the absolute position or relative position of the target object can be obtained which could have uses in the assembly sectors. A change in tag signal caused by human movement is utilized by [40] to achieve relatively high precision relative positioning. A PRDL method proposed by [41] combines deep learning with relative positioning to improve the positioning accuracy. Ranging positioning and non-ranging positioning are often utilized for two-dimensional (2-D) localization. Time of arrival (TOA), time difference of arrival (TDOA), angle of arrival (AOA), and received signal strength (RSSI) are type of ranging method utilized in the 2-D location system [42]. The use of reference was first introduced by LANDMARC and used k-NN algorithm to weigh the coordinates of tag and find the relative position of tags to be tracked based on the coordinates of reference tag [43].

A three-dimensional positioning system can achieve the spatial information of the object to be localized hence it can have a significant impact on the daily livelihood of human beings. Different techniques and algorithms like APM [44] , 3DinSAR [45], MDS [46] have been proposed which uses different methods such as minimum interrogation power and multilateral measurements, holographic atlas to find the phase difference of tags with different heights, and path loss and shielding effects respectively.

The dawn of machine learning (ML) and higher processing power has created many possibilities for data processing of RFID tags for indoor localization. A convolutional neural network (CNN) with five convolutional layers is used to determine the 3D positioning of books equipped with RFID tags on a bookshelf [47]. E. L. Berz, D. A. Tesch, and F. P. Hessel utilize ML methods based on support vector regression to estimate the location of stationary tags attached to a whiteboard [48]. A. Belay Adege, et.al proposes the integration of k-NN and Artificial Neural Networks

(ANN) to achieve a room-level classification where data is collected from three lecture rooms on the same floor [49] .

## 2.4 Dielectric of Items/Foods

RFID tags have been utilized in the tracking and supply chain management of food on numerous occasions over two decades. Walmart in 2004 AD introduced the first RFID system in its supply chain [50]. R. Jedermann, L. Ruiz-Garciab, and W. Lang used RFID tags for spatial temperature profile to monitor and analyze the refrigerated transport chain of perishable goods [51]. Abad et.al used RFID tags along with the integration of temperature and relative humidity sensors in a fresh fish logistic chain: the South African fresh hake commercial chain for the European market [52]. These works do not consider the relative dielectric of the tagged objects.

Many supplies chain items or localization targets have a high relative dielectric constant due to the water content. Water has a dielectric of 79.5 at 915 MHz at room temperature [53]. The high dielectric constant of water is also noted in literature related to the limitations of RFID tag design near the human body [54].

Table 2.1 lists the relative dielectric constant and frequency at which the respective dielectric was measured in different literature. As it is noted from Table 2.1 that the frequency for cantaloupe and pineapple doesn’t fall on the 902 – 928 MHz. This is because the available literature on the measurement of dielectric was not available for specific frequency. Since the dielectric value does not change much for the range of 150 MHz, the dielectric values at closest frequency to 902-928 MHz were utilized. Moreover, the dielectric value for cabbage is taken for blanched cabbage from [55] where the microwave blanching performed and dielectric constant measured were both at 915

MHz. Unlike blanching performed at 27 MHz, blanching at 915 MHz doesn't change the dielectric value that much. Hence the dielectric value of 72.4 is chosen for our experiment. While the object of lower dielectric material doesn't affect or attenuate the signal from RFID reader, higher dielectric materials attenuate the signal which results in improper tag readings.

Table 2.1: Dielectric Constant of some objects

| **Fruits and Vegetables** | **Relative dielectric constant ($\varepsilon_r$)** | **Frequency** |
|---|---|---|
| Water [53] | 79.5 | 915 MHz |
| Cantaloupe [56] | 63.0 | 1 GHz |
| Blanched Cabbage[55] | 72.4 | 915 MHz |
| Pineapple [57] | 76.3 | 790 MHz |
| Avocado [56] | 56 | 1 GHz |
| Plastic [58] | 2.2 | 915 MHz |

# CHAPTER 3. EXPERIMENTAL SETUP AND DATA COLLECTION

## 3.1 Introduction

This chapter presents an experimental setup used for the collection of data utilizing RFID Tags, Antennas, Reader, and other equipment.

## 3.2 Equipment and Software

The RFID system used in the setup consists of four Vulcan RFIDTM PAR90209H (RHCP) Outdoor RFID Antennas [59]. Confidex Carrier ClassicTM passive RFID tags were used which can be applied to non-metallic surfaces for identification/tracking purpose [60]. The average cost of for these tags is 50 cents per tag and can operate in the temperature -9°C to 54°C [60]. Impinj Speedway R420 4-port (FCC) Fixed Reader [61] was used to read tags using the ItemTest software [62]. The transmission power (Tx) and received sensitivity (Rx) of the antenna connected to the reader was set to 32.5 dBm and 80 dBm respectively using ItemTest software. Three different fruits and vegetables: Cantaloupe, Cabbage, and Pineapple were equipped with RFID tags to collect the location information as shown in Figure 3.1.

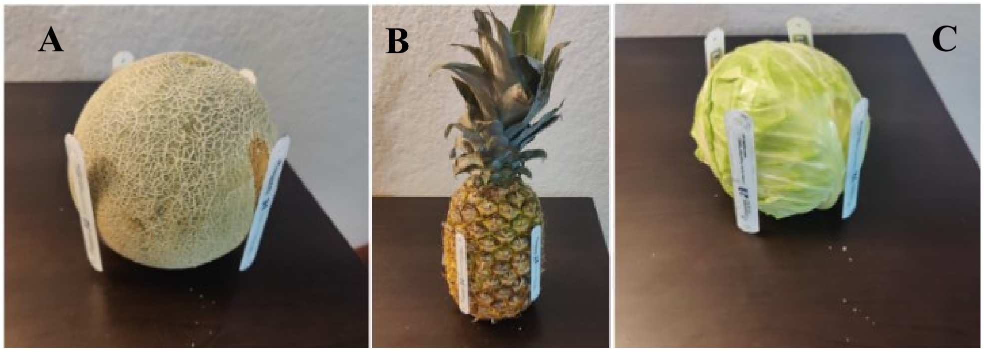


Figure 3.1: Fruits and vegetables equipped with RFID tags. (A) Cantaloupe, (B) Pineapple, and (C) Cabbage.

### 3.3 Setup

A total of 32 RFID tags were used in this experiment, four of them being tracking tags and 28 of them being reference tags. Reference tags numbered 1-16 were affixed to the smooth foam board of dimension 135 x 108 cm in an x-z plane with tags being 45 cm apart on the x-axis and 36 cm apart on the z-axis from each other. Reference tags numbered 17-28 were affixed to the flattened-out moving box of dimension 135 cm x 135 cm in the x-y plane with a tag separation of 45 cm in both the x and y-axis. An experimental setup with all equipment used in the data collection is shown in Figure 3.2. The cardboard box parallel to the floor in Figure 3.2(b) is elevated from the ground by 13 cm using additional small cardboard boxes to minimize the effect of the concrete floor on the electromagnetic properties of tags.

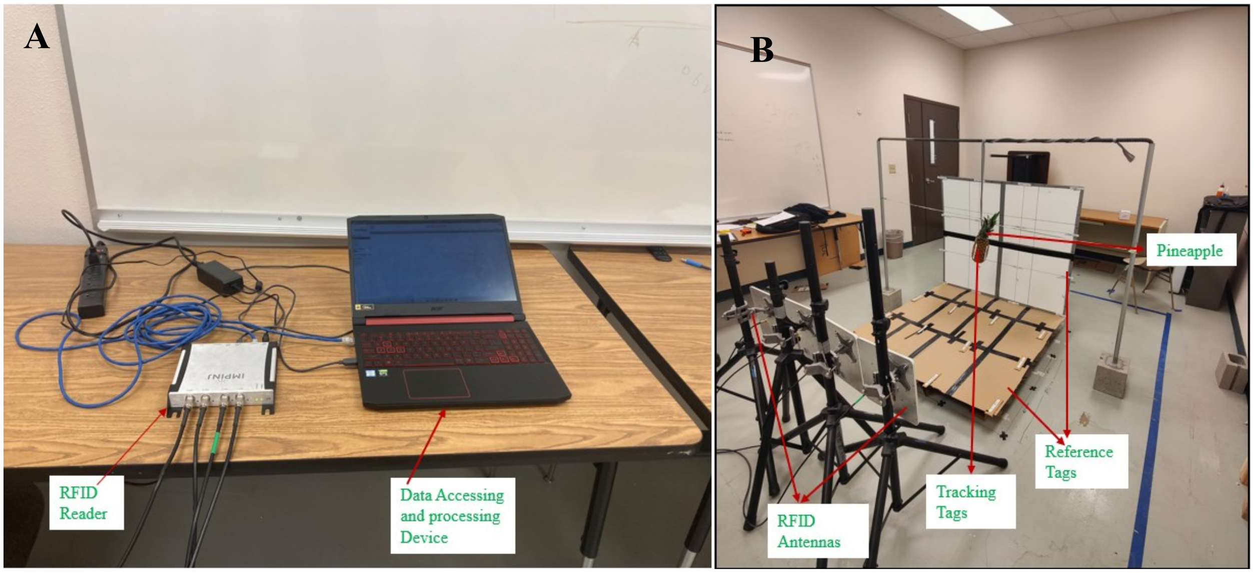


Figure 3.2: Experimental setup (A) Reading and storing location information (B) pineapple under testing.

The rest of the tags numbered 29-32 were labeled as tracking tags which were equipped on different vegetables and fruits. Two rods with sturdy bases, connected on the top by another rod, were used as an anchor to hold the different subjects under the test. Nylon fabrics were used to hold the subject from the top and to prevent the rotation to maintain fixed tracking tags' coordinates as shown in Figure 3.2(B). Four tracking tags are utilized to improve triangulation, reduce blind spots, mitigate signal interference, and to improve precision [63]. RSSI value is utilized as a metric for evaluation of indoor localization as it provides decent accuracy with relatively simple setup and low power consumption. Techniques like phase, AOA, and TOA are not utilized because with a large number of tags (tag density) these techniques can lead to computational load and potential collision issues [64]. Moreover, the prime focus of our research is to study the effect of dielectric constant on RFID indoor localization, RSSI metric is used as a preliminary focus to compute indoor localization accuracy.

### 3.4 Data Collection

While the coordinates for the tracking tags were different for each item under the test the coordinates for the reference tags are the same in all experimental setups. The fixed coordinates for the reference tags are shown in Table 3.1. Data was collected for a total of 9 minutes (540 seconds) for each setup. Data was collected for a total of 9 minutes because that ensured enough datapoints for training and testing using ML algorithms given these the ML models utilized perform better with enough datapoints to ensure better accuracy for different time of data collection. The frequency band for this data collection is from 902-928 MHz.

#### 3.4.1 Data collection for dielectric constant ($\varepsilon_r$) of 76.3

First the data is collected for a pineapple with a dielectric of 76.3. Pineapple is wrapped around a nylon fabric and then suspended from the vertical bar. Data is then collected for a total of 9 minutes. Figure 3.2(b) above shows the experimental setup for pineapple. While the coordinates for the reference tags are fixed as mentioned earlier, the changing coordinates for the tracking tags (29-32) affixed to the pineapple are listed in Table 3.2.

Table 3.1: Coordinates for reference tags

| **Reference Tag** | **X** | **Y** | **Z** |
|---|---|---|---|
| 1 | 0 | 0 | 0 |
| 2 | 45 | 0 | 0 |
| 3 | 90 | 0 | 0 |
| 4 | 135 | 0 | 0 |

| **Reference Tag** | **X** | **Y** | **Z** |
|---|---|---|---|
| 5 | 0 | 0 | 36 |
| 6 | 45 | 0 | 36 |
| 7 | 90 | 0 | 36 |
| 8 | 135 | 0 | 36 |
| 9 | 0 | 0 | 72 |
| 10 | 45 | 0 | 72 |
| 11 | 90 | 0 | 72 |
| 12 | 135 | 0 | 72 |
| 13 | 0 | 0 | 108 |
| 14 | 45 | 0 | 108 |
| 15 | 90 | 0 | 108 |
| 16 | 135 | 0 | 108 |
| 17 | 0 | 45 | 0 |
| 18 | 45 | 45 | 0 |
| 19 | 90 | 45 | 0 |
| 20 | 135 | 45 | 0 |
| 21 | 135 | 90 | 0 |
| 22 | 90 | 90 | 0 |
| 23 | 45 | 90 | 0 |
| 24 | 0 | 90 | 0 |
| 25 | 0 | 135 | 0 |

| Reference Tag | X | Y | Z |
|---|---|---|---|
| 26 | 45 | 135 | 0 |
| 27 | 90 | 135 | 0 |
| 28 | 135 | 135 | 0 |

Table 2.2: Coordinates of tracking tags affixed to pineapple.

| Tracking Tag | X | Y | Z |
|---|---|---|---|
| 29 | 95 | 62 | 66 |
| 30 | 88 | 66 | 66 |
| 31 | 80 | 59 | 66 |
| 32 | 89 | 54 | 66 |

### 3.4.2 Data collection for dielectric constant ($\varepsilon_r$) of 72.4

Next the data is collected for cabbage with dielectric of 72.4. Light weight and spherical shape of cabbage was prone to rotational motion, making it challenging to maintain the fixed tracking tag's coordinate. Data collection process is started only after the cease of rotational motion of cabbage.

Experimental setup for cabbage is shown in Figure 3.3, whereas the coordinate of tracking tags affixed to cabbage are noted in Table 3.3.

Table 3.3: Coordinates for tracking tags affixed to cabbage.

| **Tracking Tag** | **X** | **Y** | **Z** |
|---|---|---|---|
| 29 | 81 | 63 | 74 |
| 30 | 80 | 53 | 74 |
| 31 | 88 | 54 | 74 |
| 32 | 91 | 61 | 74 |

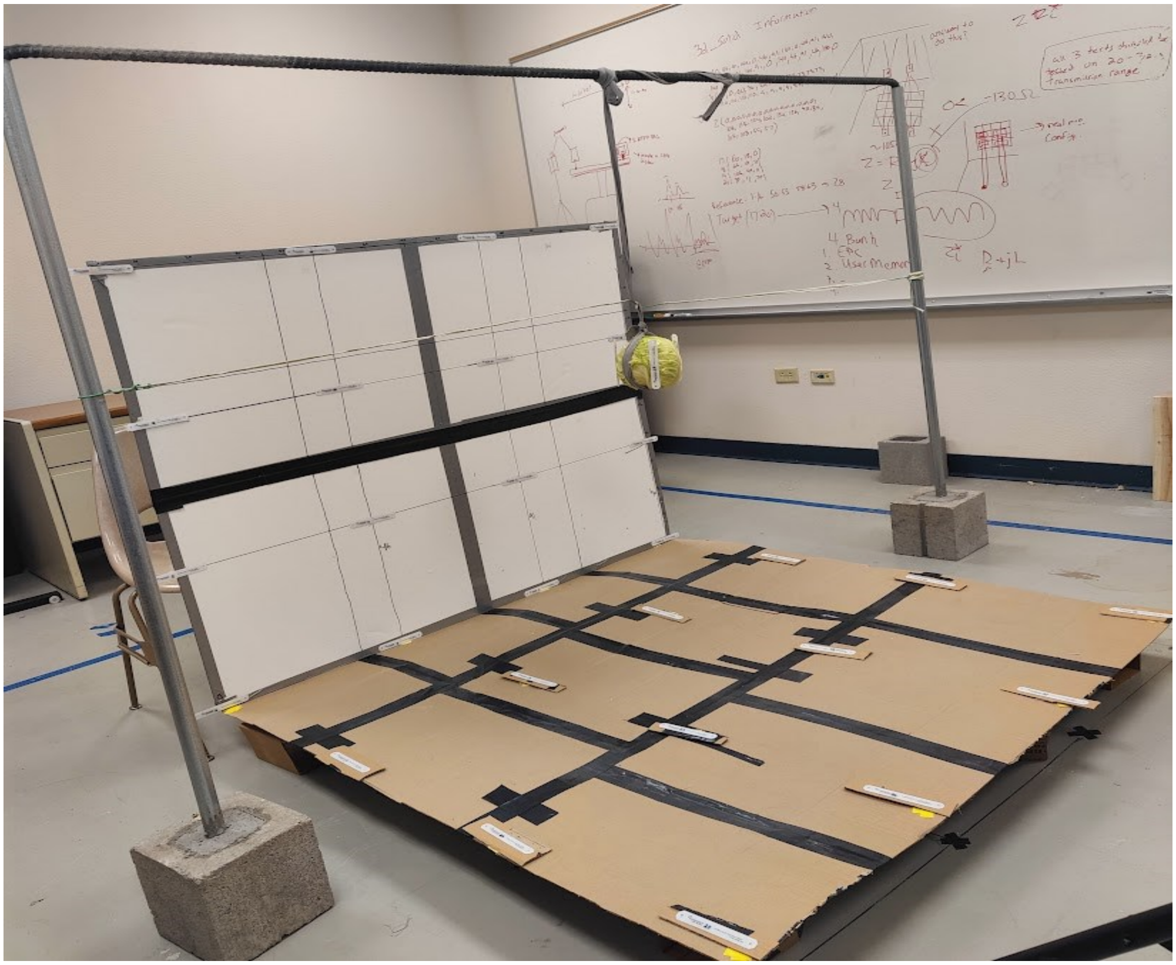

Figure 3.3: Experimental Setup for Cabbage under testing

### 3.4.3 Data collection for dielectric constant ($\varepsilon_r$) of 63.0

Finally, the data is collected for cantaloupe which has a dielectric constant value of 63.0. An experimental setup for data collection of cantaloupes is shown in Figure 3.4, whereas coordinates of tracking tags affixed to cantaloupe are listed in Table 3.4**.**

Table 3.4: Coordinates of tracking tags affixed to cantaloupe.

| **Tracking Tag** | **X** | **Y** | **Z** |
|---|---|---|---|
| 29 | 81 | 63 | 74 |
| 30 | 80 | 53 | 74 |
| 31 | 88 | 54 | 74 |
| 32 | 91 | 61 | 74 |

Figure 3.4: Experimental setup with cantaloupe under testing

### 3.5 Description of data

Sample raw data collected from the experiment is shown is Table 3.5. Here, Timestamp is the time at which the tags are read, EPC is the unique identifier for each tag numbered from 1-32, Antenna is the antenna that reads the respective tag, and RSSI is the strength of signal in dBm associated to the respective tag.

Table 3.5: Sample of raw data collected.

| **Timestamp** | **EPC** | **Antenna** | **RSSI** |
|---|---|---|---|
| 2022-01-31T22:10:40.8410320-07:00 | 30 | 1 | -43 |
| 2022-01-31T22:10:40.8419730-07:00 | 13 | 3 | -48 |
| 2022-01-31T22:10:40.8435950-07:00 | 12 | 4 | -49.5 |
| 2022-01-31T22:10:40.8450660-07:00 | 32 | 1 | -48 |
| 2022-01-31T22:10:40.8456140-07:00 | 7 | 2 | -46.5 |
| 2022-01-31T22:10:40.8461580-07:00 | 6 | 1 | -47 |
| 2022-01-31T22:10:40.8490990-07:00 | 8 | 4 | -48.5 |
| 2022-01-31T22:10:40.8813860-07:00 | 15 | 1 | -47 |
| 2022-01-31T22:10:40.8853150-07:00 | 16 | 1 | -48 |
| 2022-01-31T22:10:40.8919010-07:00 | 31 | 3 | -49 |
| 2022-01-31T22:10:40.8934320-07:00 | 5 | 1 | -49.5 |
| 2022-01-31T22:10:41.2565990-07:00 | 29 | 2 | -46.5 |

# CHAPTER 4. DATA PROCESSING AND ANALYSIS OF DATA

## 4.1 General

In this chapter, the processing and feature engineering performed in the data, ML algorithms utilized, and analysis of the results is presented. The processed data is analyzed using three supervised ML algorithms: (i) k-NN, (ii) XgBoost, and (iii) decision tree. Python programming is utilized to perform the analysis.

## 4.2 Data preprocessing and feature engineering

### 4.2.1 Data preprocessing

Raw data consisted of four columns and 24,000 rows on average. The columns of the data set are expanded to a total of 13 columns including the columns with coordinate information for each EPC of the tag. Coordinates information is first stored in the NumPy array and then merged into the entire collected dataset which is converted to pandas' data frame. A sample dataset is shown in Table 4.1, where $EPC_{RT}$, $RSSI_X$ , $X_{RT}$, $Y_{RT}$, $Z_{RT}$ are the EPC, RSSI, x-coordinate, y-coordinate, and z-coordinate of the reference tags, whereas $Ant_X$ and $Ant_Y$ are the respective antenna that read reference and tracking tags. $EPC_{TT}$, $RSSI_Y$ , $X_{TT}$, $Y_{TT}$, $Z_{TT}$ are the EPC, RSSI, x-coordinate, y-coordinate, and z-coordinate of the tracking tags.

### 4.2.2 Feature engineering

The time column in the raw data is transformed. A new column Seconds is made which is the each second the data is recorded for both reference and tracking tag. This feature is engineered to protect the time information when analyzing data with ML algorithms. This feature basically

Table 4.1: A sample data after preprocessing and feature engineering.

| $EPC_{RT}$ | $Ant_X$ | $RSSI_X$ | $Seconds$ | $EPC_{TT}$ | $Ant_Y$ | $RSSI_Y$ | $X_{TT}$ | $Y_{TT}$ | $Z_{TT}$ | $X_{RT}$ | $Y_{RT}$ | $Z_{RT}$ |
|---|---|---|---|---|---|---|---|---|---|---|---|---|
| 10 | 3 | -63.0 | 539.0 | 29 | 1 | -66.5 | 95 | 62 | 66 | 45 | 0 | 72 |
| 10 | 3 | -63.0 | 539.0 | 31 | 2 | -66.0 | 80 | 59 | 66 | 45 | 0 | 72 |
| 10 | 3 | -63.0 | 539.0 | 31 | 2 | -66.5 | 80 | 59 | 66 | 45 | 0 | 72 |
| 8 | 3 | -61.5 | 539.0 | 31 | 2 | -67.0 | 80 | 59 | 66 | 135 | 0 | 36 |
| 8 | 2 | -61.5 | 539.0 | 32 | 2 | -67.0 | 89 | 54 | 66 | 135 | 0 | 36 |
| 15 | 2 | -62.5 | 539.0 | 32 | 3 | -66.5 | 89 | 54 | 66 | 90 | 0 | 108 |
| 6 | 4 | -62.0 | 540.0 | 30 | 3 | -65.5 | 88 | 66 | 66 | 45 | 0 | 36 |
| 6 | 4 | -62.0 | 540.0 | 30 | 3 | -67.5 | 88 | 66 | 66 | 45 | 0 | 36 |
| 6 | 4 | -62.0 | 540.0 | 30 | 4 | -66.5 | 88 | 66 | 66 | 45 | 0 | 36 |
| 6 | 4 | -62.0 | 540.0 | 30 | 4 | -66.5 | 88 | 66 | 66 | 45 | 0 | 36 |
| 6 | 4 | -62.0 | 540.0 | 31 | 4 | -64.5 | 80 | 59 | 66 | 45 | 0 | 36 |

makes it easy to predict the coordinate of the tracking tag for each second which allows us to track objects in real time. This column ranges from value of 1 to 940, 1 indicating first second of data collection and 940 the last second.

#### 4.2.3 Splitting dataset

Now the dataset is split into training and testing sets without data shuffling to have data in time order of seconds. Training dataset included columns $EPC_{RT}$, $RSSI_X$ , $X_{RT}$, $Y_{RT}$, $Z_{RT}$, $Ant_X$, $Ant_Y$, $RSSI_Y$, and $Seconds$. The test set is taken to be $EPC_{TT}$ which is the EPC of the tracking tag. The training dataset is taken to be 80% of the total data and 20% is allocated as testing dataset. Since the data is not shuffled, the training set includes data for 80% which is for the first 432 seconds of data collection.

### 4.3. Data analysis with Supervised ML algorithms

Now, different ML algorithms like k-NN, XgBoost, and Decision tree were used to classify the test set. Data was analyzed using python programming language in Jupiter notebook using google co-lab free version which gives access to cloud computing with CPU of single or dual core processor, RAM of 12 GB and storage of 100 GB.

#### 4.3.1 Analysis with k-NN algorithm

A k-NN algorithm with five neighbors and distance as a weight is utilized to obtain training and testing accuracy. In scikit-learn's k-Nearest Neighbors (kNN) algorithm, the default distance metric used to measure the distance between data points is the Euclidean distance. The code below is utilized for this process. The average CPU time in this process for convergence of data is 71 seconds. The results obtained for training and testing accuracy for different dielectric constants are listed in Table 4.2.

```
%%time
```

```
# Perform kNN

from sklearn.neighbors import KNeighborsClassifier

kNN = KNeighborsClassifier(n_neighbors=5, weights='distance') # Specify k = n_neighbors

kNN.fit(z_X_train,y_train)

print('Training accuracy: ', kNN.score(z_X_train,y_train))

print('Testing accuracy: ', kNN.score(z_X_test,y_test))
```

Table 4.2: localization accuracy using k-NN Algorithm

| **Fruits and Vegetables** | **Relative dielectric constant ($\varepsilon_r$)** | **Training Accuracy** | **Testing Accuracy** |
|---|---|---|---|
| Cantaloupe | 63.0 | 87.7 % | 52.15% |
| Cabbage | 72.4 | 96.9% | 77.7% |
| Pineapple | 76.3 | 96.34% | 72.73% |

### 4.3.2 Analysis with XGBoost algorithm

An XGBoost algorithm with XGBClassifier is utilized to obtain the testing and training accuracy. The code below is utilized in this process. The average CPU time in this process for convergence of data is 15 seconds. The results obtained for training and testing accuracy for different dielectric constants are listed in Table 4.3.

```
%%time

from sklearn.model_selection import train_test_split

X_train, X_test, y_train, y_test = train_test_split(X,y,test_size=1/5,shuffle=False) # 20% test no shuffling

from xgboost import XGBClassifier

xgb = XGBClassifier()

xgb.fit(X_train, y_train)
```

Table 4.3: Localization accuracy using XGBoost algorithm.

| **Fruits and Vegetables** | **Relative dielectric constant ($\varepsilon_r$)** | **Training Accuracy** | **Testing Accuracy** |
|---|---|---|---|
| Cantaloupe | 63.0 | 57.1 % | 54.36 % |
| Cabbage | 72.4 | 79.92 % | 78.34 % |
| Pineapple | 76.3 | 78.3 % | 76.9 % |

### 4.3.3 Analysis with Decision Tree algorithm

An decision tree algorithm with DecisionTreeClassifier is utilized to obtain the testing and training accuracy. The code below is utilized in this process. The average CPU time in this process for convergence of data is 10 seconds. The results obtained for training and testing accuracy for different dielectric constants are listed in Table 4.4.

```
# Decision Trees

%%time

from sklearn.tree import DecisionTreeClassifier

class_tree = DecisionTreeClassifier()

class_tree.fit(X_train, y_train)

print(class_tree)
```

Table 4.4: Localization accuracy using decision tree algorithm.

| **Fruits and Vegetables** | **Relative dielectric constant ($\varepsilon_r$)** | **Training Accuracy** | **Testing Accuracy** |
|---|---|---|---|
| Cantaloupe | 63.0 | 87.7 % | 48.8 % |
| Cabbage | 72.4 | 96.89 % | 74.5 % |
| Pineapple | 76.3 | 96.34 % | 68.3 % |

### 4.4. Results and Analysis

Figure 4.1 shows the results obtained from processed data with three different supervised ML algorithms k-NN, Decision tree, and XGBoost. Figure 4.2 shows the scatter plot of test accuracy for the aforementioned ML algorithms for different values of relative dielectric constants. We can observe from Figure 4.1 that k-NN and the Decision tree algorithm are quite overfitting, but XGBoost performs well for all the items under the test. From Figure 4.2 we can see that the dielectric value of the item under the test has a significant effect on indoor localization using RSSI-based indoor localization.

The test accuracy for cantaloupe whose dielectric value is quite low has a test accuracy of 54.3 % with the best-performing algorithm. Whereas the test accuracy of pineapple and cabbage, which has relatively close dielectric value, stands at 76.9% and 78.34% respectively with the same XGBoost algorithm. For pineapple and cabbage which have a higher dielectric constant, these generally seem to have a higher localization accuracy. We suspect that increasing dielectric constant increases localization accuracy, but additional testing with precise dielectric values and uniform object size is required.

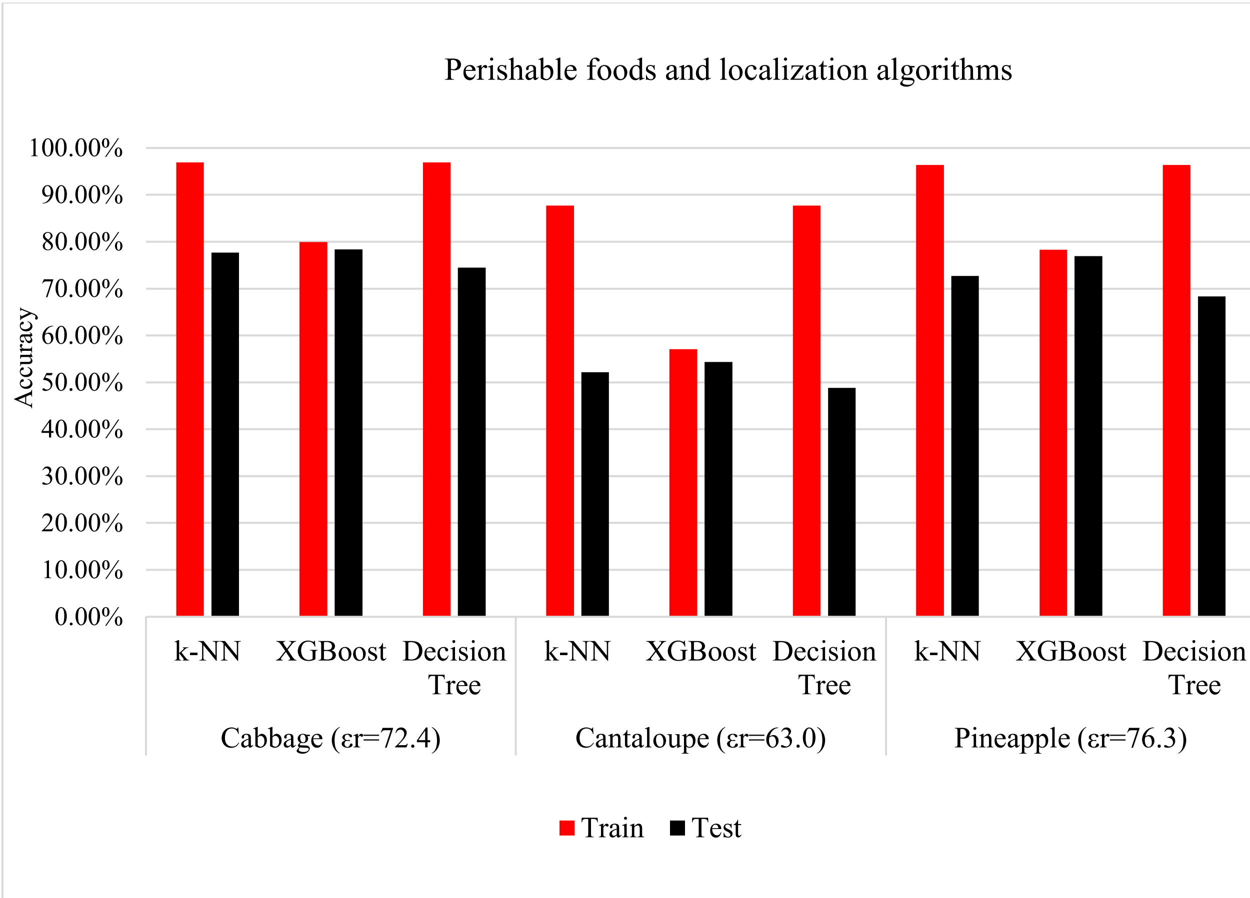


Figure 4.1: Train and test accuracy for indoor localization of cabbage, cantaloupe, and pineapple.

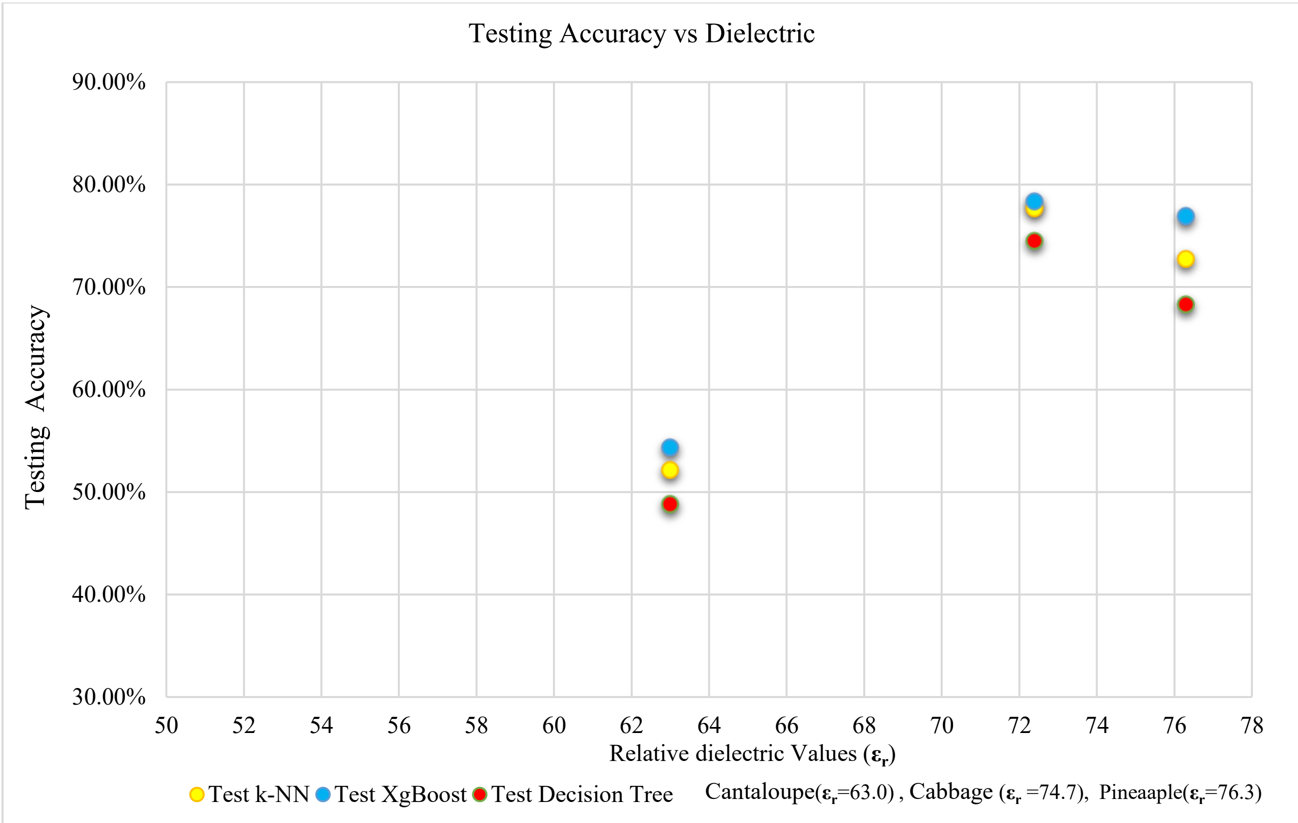


Figure 4.2: Testing Accuracy vs Dielectric constant

# CHAPTER 5. CONCLUSION

## 5.1. Conclusion

In this research we delved into one of the prominent material properties which is the dielectric constant and its effect on RSSI-based indoor localization using RFID systems. Three ML algorithms: k-NN, XGBoost, and decision tree are used to classify three different items (cantaloupe, cabbage, and pineapple) equipped with passive RFID tags in real-time using time information as one of the feature engineering. It is seen that the dielectric properties of items under the test have a significant effect on indoor localization accuracy. This research offers new insight into the effect of dielectric constant and how it should be considered an important feature while developing indoor localization systems.

## 5.2. Recommendation for future research

In supply chain management, these items (fruits and vegetables) are often not exposed by themselves but are usually boxed, wrapped, and sometimes even frozen. Further research with utilization of supply chain setup to collect data would be more useful to improve visibility, cold chain monitoring, and automated check in and check out.

RFID (Radio Frequency Identification) tags are generally more resource-efficient compared to traditional barcode labels. RFID tags consume minimal power during operation, and many passive RFID and especially chip less tags do not require a battery which ensures their sustainability towards the environment. As RFID tags become more widespread, industries are likely to develop recycling programs for end-of-life tags. This will further reduce the environmental impact.

Future work of training and testing of the dataset should be focused on utilizing instead of averaging RSSI for each second of data collection. When rounding to nearest second can lead to loss of datapoints which can be crucial when developing real time location systems. This research focused on the static environment so the time data didn't play a big role in the accuracy of the system but when developing dynamic indoor localization systems this feature will be prominent in prediction of the tracking coordinates.

Based on the findings from this research, a material property such as dielectric has prominent impact in the RFID indoor localization system. However, further research is required to fully understand the impact in indoor localization with consideration of different nuances. The following are some of the nuanced research areas for future studies:

1. Use of precise dielectric values and uniform object.
2. Study the impact of phase angle along with RSSI and its impact on the indoor localization accuracy.
3. Indoor localization with dynamic of the object to localized can be studied.
4. Research into other ML algorithms like random forests, naïve bias, support vector machine, and so on.
5. Study the impact of varying accuracy on the indoor localization with varying values of transfer and receive power.

## REFERENCES


[1] F. Zafari, A. Gkelias, and K. K. Leung, "A survey of indoor localization systems and technologies," *IEEE Communications Surveys & Tutorials*, vol. 21, no. 3, pp. 2568–2599, 2019.

[2] R. Weinstein, "RFID: a technical overview and its application to the enterprise," *IT professional*, vol. 7, no. 3, pp. 27–33, 2005.

[3] L. Gavoni, "RFID Exploitation and Countermeasures," *arXiv preprint arXiv:2110.00094*, 2021.

[4] Admin, "The History of RFID Technology," *RFID JOURNAL*, Jan. 16, 2005. https://www.rfidjournal.com/the-history-of-rfid-technology (accessed Jun. 23, 2023).

[5] E. Ilie-Zudor, Z. Kemeny, P. Egri, and L. Monostori, "The RFID technology and its current applications," in *Conference Proceedings of the Modern Information Technology in the Innovation Processes of the Industrial Enterprises (MITIP)*, 2006, pp. 29–36.

[6] M. Abdelkarim, S. Naoui, C. Essid, and A. Gharsallah, "A New Solution for Car Parking RFID Reader," in *2019 IEEE 19th Mediterranean Microwave Symposium (MMS)*, IEEE, 2019, pp. 1–4.

[7] C. M. Ramya and R. B. Rani, "Miniaturized Spidron Fractal Wide-Slot Antenna for 5.8 GHz Active Radio Frequency Identification Tag Applications," *Iranian Journal of Science and Technology, Transactions of Electrical Engineering*, vol. 46, no. 4, pp. 935–942, 2022.

[8] S. Preradovic, N. C. Karmakar, and I. Balbin, “RFID transponders,” *IEEE microwave magazine*, vol. 9, no. 5, pp. 90–103, 2008.

[9] T. T. Electronics, “RFID: The Technology Making Industries Smarter.” https://blog.ttelectronics.com/rfid-technology (accessed Jun. 24, 2023).

[10] E. Brynjolfsson and A. Mcafee, “Artificial intelligence, for real,” *Harvard business review*, vol. 1, pp. 1–31, 2017.

[11] R. Abduljabbar, H. Dia, S. Liyanage, and S. A. Bagloee, “Applications of artificial intelligence in transport: An overview,” *Sustainability*, vol. 11, no. 1, p. 189, 2019.

[12] H. Malik, S. Srivastava, Y. R. Sood, and A. Ahmad, *Applications of Artificial Intelligence Techniques in Engineering: SIGMA 2018, Volume 2*, vol. 697. Springer, 2018.

[13] S. Reddy, S. Allan, S. Coghlan, and P. Cooper, “A governance model for the application of AI in health care,” *Journal of the American Medical Informatics Association*, vol. 27, no. 3, pp. 491–497, 2020.

[14] N. C. Eli-Chukwu, “Applications of artificial intelligence in agriculture: A review,” *Engineering, Technology & Applied Science Research*, vol. 9, no. 4, pp. 4377–4383, 2019.

[15] P. Van Esch, J. S. Black, and J. Ferolie, “Marketing AI recruitment: The next phase in job application and selection,” *Computers in Human Behavior*, vol. 90, pp. 215–222, 2019.

[16] A. Haibi, K. Oufaska, K. E. Yassini, M. Boulmalf, and M. Bouya, “Systematic Mapping Study on RFID Technology,” *IEEE Access*, vol. 10, pp. 6363–6380, 2022, doi: 10.1109/ACCESS.2022.3140475.

[17] S. Md. Shahid, “Use of RFID technology in libraries: a new approach to circulation, tracking, inventorying, and security of library materials,” *Library Philosophy and Practice*, vol. 8, no. 1, 2005, Accessed: Mar. 10, 2023. [Online]. Available: https://link.gale.com/apps/doc/A139169928/AONE?u=anon~f748a7f6&sid=googleScholar&xid=39903c79

[18] Y. Álvarez López, J. Franssen, G. Álvarez Narciandi, J. Pagnozzi, I. González-Pinto Arrillaga, and F. Las-Heras Andrés, “RFID Technology for Management and Tracking: e-Health Applications,” *Sensors*, vol. 18, no. 8, p. 2663, Aug. 2018, doi: 10.3390/s18082663.

[19] A. A. Norman, N. Md Nasir, and M. Azmi, “The users perceptions and opportunities in Malaysia in introducing RFID system for Halal food tracking,” *Computer Journal WSEAS Transactions on Information Science and Applications*, vol. 5, no. 5, pp. 843–852, 2008.

[20] G. Oguntala, R. Abd-Alhameed, S. Jones, J. Noras, M. Patwary, and J. Rodriguez, “Indoor location identification technologies for real-time IoT-based applications: An inclusive survey,” *Computer Science Review*, vol. 30, pp. 55–79, 2018.

[21] K. C. A. Khanzode and R. D. Sarode, “Advantages and disadvantages of artificial intelligence and machine learning: A literature review,” *International Journal of Library & Information Science (IJLIS)*, vol. 9, no. 1, p. 3, 2020.

[22] S. Athmaja, M. Hanumanthappa, and V. Kavitha, “A survey of machine learning algorithms for big data analytics,” in *2017 International conference on innovations in information, embedded and communication systems (ICIIECS)*, IEEE, 2017, pp. 1–4.

[23] B. Mahesh, “Machine learning algorithms-a review,” *International Journal of Science and Research (IJSR).[Internet]*, vol. 9, pp. 381–386, 2020.

[24] A. Géron, “Hands-on machine learning with scikit-learn and tensorflow: Concepts,” *Tools, and Techniques to build intelligent systems*, 2017.

[25] C. K. H. Lee, G. T. S. Ho, K. L. Choy, and G. K. H. Pang, “A RFID-based recursive process mining system for quality assurance in the garment industry,” *International journal of production research*, vol. 52, no. 14, pp. 4216–4238, 2014.

[26] X. Wang, “Tennis robot design via Internet of Things and deep learning,” *IEEE Access*, vol. 9, pp. 127460–127470, 2021.

[27] E. Perret, “Technologie RFID sans puce,” *La Revue de l’électricité et de l’électronique*, 2017.

[28] C. Herrojo, F. Paredes, J. Mata-Contreras, and F. Martín, “Chipless-RFID: A review and recent developments,” *Sensors*, vol. 19, no. 15, p. 3385, 2019.

[29] J. Xi and T. T. Ye, “A manufacture-friendly multi-layer RFID tag antenna design,” in *2013 7th European Conference on Antennas and Propagation (EuCAP)*, IEEE, 2013, pp. 3238–3241.

[30] A. S. A. Jalal, “Passive RFID Tags,” *Wulfenia Journal*, vol. 22, no. 12, pp. 415–435, 2015.

[31] “Understanding RFID and RFID Operating Ranges,” Mar. 27, 2017. https://blog.acdist.com/understanding-rfid-and-rfid-operating-ranges (accessed Jun. 30, 2023).

[32] A. A. Mbacke, N. Mitton, and H. Rivano, “A survey of RFID readers anticollision protocols,” *IEEE Journal of Radio Frequency Identification*, vol. 2, no. 1, pp. 38–48, 2018.

[33] Y. Rouchdi, K. El Yassini, and K. Oufaska, “Resolving security and privacy issues in radio frequency identification middleware,” *International Journal of Innovative Science, Engineering & Technology (IJISET)*, vol. 5, no. 2, pp. 2348–7968, 2018.

[34] Y. Rouchdi, K. El Yassini, and K. Oufaska, “Complex event processing and role-based access control implementation in ESN middleware,” in *Innovations in Smart Cities and Applications: Proceedings of the 2nd Mediterranean Symposium on Smart City Applications 2*, Springer, 2018, pp. 966–975.

[35] T. Noergaard, *Demystifying embedded systems middleware*. Elsevier, 2010.

[36] M. C. O’Connor, “RFID is key to Car Clubs’ Success,” *RFID Journal*, 2008.

[37] T. Van Deursen, S. Mauw, and S. Radomirović, “Untraceability of RFID protocols,” in *Information Security Theory and Practices. Smart Devices, Convergence and Next Generation Networks: Second IFIP WG 11.2 International Workshop, WISTP 2008, Seville, Spain, May 13-16, 2008. Proceedings 2*, Springer, 2008, pp. 1–15.

[38] M. Bouet and A. L. dos Santos, “RFID tags: Positioning principles and localization techniques,” in *2008 1st IFIP Wireless Days*, Dubai, United Arab Emirates: IEEE, Nov. 2008, pp. 1–5. doi: 10.1109/WD.2008.4812905.

[39] J. Zhou and J. Shi, “RFID localization algorithms and applications—a review,” *J Intell Manuf*, vol. 20, no. 6, pp. 695–707, Dec. 2009, doi: 10.1007/s10845-008-0158-5.

[40] G. Wang *et al.*, “HMRL: Relative localization of RFID tags with static devices,” in *2017 14th Annual IEEE International Conference on Sensing, Communication, and Networking (SECON)*, IEEE, 2017, pp. 1–9.

[41] L. Shen, Q. Zhang, J. Pang, H. Xu, and P. Li, “PRDL: Relative localization method of RFID tags via phase and RSSI based on deep learning,” *IEEE access*, vol. 7, pp. 20249–20261, 2019.

[42] K. K. Chintalapudi, A. Dhariwal, R. Govindan, and G. Sukhatme, “Ad-hoc localization using ranging and sectoring,” in *IEEE INFOCOM 2004*, IEEE, 2004, pp. 2662–2672.

[43] L. M. Ni, Y. Liu, Y. C. Lau, and A. P. Patil, “LANDMARC: Indoor location sensing using active RFID,” in *Proceedings of the First IEEE International Conference on Pervasive Computing and Communications, 2003.(PerCom 2003).*, IEEE, 2003, pp. 407–415.

[44] A. Almaaitah, K. Ali, H. S. Hassanein, and M. Ibnkahla, “3D passive tag localization schemes for indoor RFID applications,” in *2010 IEEE International Conference on Communications*, IEEE, 2010, pp. 1–5.

[45] L. Qiu, Z. Huang, N. Wirström, and T. Voigt, "3DinSAR: Object 3D localization for indoor RFID applications," in *2016 IEEE International Conference on RFID (RFID)*, IEEE, 2016, pp. 1–8.

[46] F. Tlili, N. Hamdi, and A. Belghith, "Accurate 3D localization scheme based on active RFID tags for indoor environment," in *2012 IEEE International Conference on RFID-Technologies and Applications (RFID-TA)*, IEEE, 2012, pp. 378–382.

[47] S. Cheng, S. Wang, W. Guan, H. Xu, and P. Li, "3DLRA: An RFID 3D Indoor Localization Method Based on Deep Learning," *Sensors*, vol. 20, no. 9, p. 2731, May 2020, doi: 10.3390/s20092731.

[48] E. L. Berz, D. A. Tesch, and F. P. Hessel, "RFID indoor localization based on support vector regression and k-means," in *2015 IEEE 24th International Symposium on Industrial Electronics (ISIE)*, Buzios, Rio de Janeiro, Brazil: IEEE, Jun. 2015, pp. 1418–1423. doi: 10.1109/ISIE.2015.7281681.

[49] A. Belay Adege, Y. Yayeh, G. Berie, H. Lin, L. Yen, and Y. R. Li, "Indoor localization using K-nearest neighbor and artificial neural network back propagation algorithms," in *2018 27th Wireless and Optical Communication Conference (WOCC)*, Hualien: IEEE, Apr. 2018, pp. 1–2. doi: 10.1109/WOCC.2018.8372704.

[50] S. J. Lee and A. M. Rahman, "Intelligent packaging for food products," in *Innovations in food packaging*, Elsevier, 2014, pp. 171–209.

[51] R. Jedermann, L. Ruiz-Garcia, and W. Lang, “Spatial temperature profiling by semi-passive RFID loggers for perishable food transportation,” *Computers and electronics in Agriculture*, vol. 65, no. 2, pp. 145–154, 2009.

[52] E. Abad *et al.*, “RFID smart tag for traceability and cold chain monitoring of foods: Demonstration in an intercontinental fresh fish logistic chain,” *Journal of food engineering*, vol. 93, no. 4, pp. 394–399, 2009.

[53] Y. A. Gezahegn *et al.*, “Dielectric properties of water relevant to microwave assisted thermal pasteurization and sterilization of packaged foods,” *Innovative Food Science & Emerging Technologies*, vol. 74, p. 102837, 2021.

[54] C. M. Roberts, “Radio frequency identification (RFID),” *Computers & security*, vol. 25, no. 1, pp. 18–26, 2006.

[55] J. Xu, B. Wang, and Y. Wang, “Electromagnetic fields assisted blanching—Effect on the dielectric and physicochemical properties of cabbage,” *Journal of Food Process Engineering*, vol. 42, no. 8, p. e13294, 2019.

[56] S. O. Nelson, “Dielectric spectroscopy of fresh fruits and vegetables,” in *2005 IEEE Instrumentationand Measurement Technology Conference Proceedings*, IEEE, 2005, pp. 360–364.

[57] A. Kaewrawang, S. Swatdiponphallop, and A. Siritaratiwat, “Study on complex permittivity of tropical thai fruits,” *Journal of Applied Sciences*, vol. 7, no. 7, pp. 1009–1012, 2007.

[58] G. Deshazer, M. Hagmann, D. Merck, J. Sebek, K. B. Moore, and P. Prakash, "Computational modeling of 915 MHz microwave ablation: Comparative assessment of temperature-dependent tissue dielectric models," *Medical Physics*, vol. 44, no. 9, pp. 4859–4868, 2017.

[59] "Vulcan RFID™ PAR90209H (RHCP) Outdoor RFID Antenna (FCC)." https://www.atlasrfidstore.com/vulcan-rfid-par90209h-rhcp-outdoor-rfid-antenna-fcc/ (accessed Mar. 10, 2023).

[60] "Confidex Carrier Classic™ RFID Tag." https://www.atlasrfidstore.com/confidex-carrier-classic-rfid-tag/ (accessed Mar. 10, 2023).

[61] "Impinj ItemTest Software – Impinj Support Portal." https://support.impinj.com/hc/en-us/articles/204059593-Impinj-ItemTest-Software (accessed Mar. 10, 2023).

[62] "Impinj Speedway R420 Four Port RFID Reader with FREE Antennas." http://www.rfidsolutionsinc.com/impinj-speedway-r420-four-port-rfid-reader-with-free-antennas (accessed Mar. 10, 2023).

[63] B. Durtschi, M. Mahat, M. Mashal, and A. Chrysler, "Preliminary Analysis of RFID Localization System for Moving Precast Concrete Units using Multiple-Tags and Weighted Euclid Distance k-NN algorithm," in *2021 IEEE International Conference on RFID (RFID)*, Atlanta, GA, USA: IEEE, Apr. 2021, pp. 1–8. doi: 10.1109/RFID52461.2021.9444370.

[64] A. Billa, I. Shayea, A. Alhammadi, Q. Abdullah, and M. Roslee, “An overview of indoor localization technologies: Toward IoT navigation services,” in *2020 IEEE 5th International Symposium on Telecommunication Technologies (ISTT)*, IEEE, 2020, pp. 76–81.

# APPENDICES

## APPENDIX A: Confidex RFID Tag Datasheet

CONFIDEX

# PRODUCT DATASHEET

## Confidex Carrier Tough Slim™

Durable tag solution for reliable plastic container and returnable transit item tracking.

### ELECTRICAL SPECIFICATION

**Device type**
UHF RFID / EPCglobal Gen2v2

**Operational frequency**
Global 865-928 MHz

**IC type**
Impinj Monza 4QT™
Impinj Monza 4E™ (upon special request)

**Memory configuration**
With Monza 4QT: EPC 128 bit; User 512 bit; TID 96 bit
With Monza 4E: EPC 496 bit; User 128 bit; TID 96 bit

**EPC memory content**
Unique number encoded as a default

**Read range (2W ERP)***
On plastic up to 12 m / 40 ft

**Applicable surface materials***
Non-metallic surfaces.

* Read ranges are theoretical values that are calculated for non reflective environment, in where antennas with optimum directivity are used with maximum allowed operating power according to ETSI EN 302 208 (2W ERP). Different surface materials may have an effect on performance.

### MECHANICAL SPECIFICATION

**Tag encapsulation**
Scratch and bending-resistant engineering plastic

**Background adhesive**
High performance acrylic adhesive specifically for low surface energy plastics

**Weight**
1 g

**Delivery format**
Single

**Amount in box**
Inner box 100 pcs
Outer box 1000 pcs

**Tag dimensions**
122 x 18 x 2 mm / 4.80 x 0.71 x 0.08 in

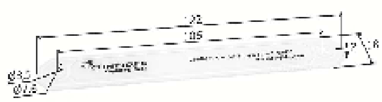


### ENVIRONMENTAL RESISTANCE

**Operating temperature**
-35°C to +85°C / -31°F to +185°F

**Ambient temperature**
-35°C to +85°C / -31°F to +185°F

**Water resistance**
IP68

**Washing resistance**
Excellent tolerance against industrial washing processes

**Chemical resistance**
No physical or performance changes in:
- 168h Salt water (salinity 10%) exposure
- 168h NaOH (10%, pH 13) exposure
- 168h Motor oil exposure
- 168h Sulfuric acid (10%, pH 2) exposure

**Storage condition**
1 year in +20°C / 50% RH (shelf life for adhesive)

**Expected lifetime**
Years in normal operating conditions

*Values in the table are the best recommendations; resistance against environmental conditions depends on the combination of all influencing factors, exposure duration and chemical concentrations. Thus, product's final suitability for certain environmental conditions is recommended to be tested. Contact Confidex for more specific information.*

1/2


11-2019

PRODUCT DATASHEET

## PERSONALIZATION OPTIONS

**Pre-encoding**

- Customer specific encoding of EPC or user memory. Locking permanently or with password.

**Customized printing**

- Customer specific layout including logo, text, numbers, barcodes etc.

## INSTALLATION INSTRUCTIONS

Confidex Carrier Tough Slim™ polarization is along the longest dimension of the tag. This should be taken into account when linear reader antennas are used.


When selecting the location ensure the following

- Select a smooth surface without uneven areas below tag
- Avoid touching the background adhesive

When mounting the label with its adhesive, clean and dry the surface for obtaining the maximum bond strength. Typical cleaning solvents are heptane for oily surfaces and isopropyl alcohol for plastics. Use reagent grade solvents since common household materials like rubbing alcohol frequently contain oils to minimize the drying effect on skin and can interfere with the performance of adhesive. Carefully read and follow the manufacturer's precautions and directions for use when working with solvents. Do not-re-attach tags as adhesion will suffer.

Ideal application temperature is from +21°C to +38°C (+70°F to +100°F), bond strength can be improved with firm application pressure and moderate heating up to +54°C (+130°F). Application at temperatures below 10°C (50°F) is not recommended.

Confidex Carrier Tough Slim™ can also be attached mechanically with:

- M3 Screws
- 3 mm Pop rivets

In harsh conditions mechanical fixing is always recommended.

## ORDER INFORMATION

**Product number:** 3001440
**Product name:** Confidex Carrier Tough Slim™ M4QT

Following products are available upon special request:
**Product number:** 3001489
**Product name:** Confidex Carrier Tough Slim™ M4E

For other versions, additional information and technical support contact Confidex Ltd.

## APPENDIX B: Vulcan RFID Antennas datasheet

PRODUCT SPEC SHEET

VULCAN RFID™

Product Family | Circularly Polarized RFID Antenna (902-928 Mhz)
Product Code | VUL-PAR90209H-FNF

# PAR90209H OUTDOOR RFID ANTENNA

The **Vulcan RFID™ PAR90209H (RHCP) Outdoor RFID Antenna** is a durable and low-profile antenna made for outdoor environments.

This circularly polarized antenna provides reception and transmission of signals in the 902-928 MHz frequency band with extremely low VSWR and axial ratios, allowing users to achieve the maximum performance for an antenna of this type.

The **Vulcan RFID™ PAR90209H** is housed in an **IP67 rated enclosure** denoting its rugged and weatherproof design, and is UL 94-V2 rated for flammability. Additionally, the heavy duty radome enclosure is capable of being directly wall-mounted. This antenna is also offered in a left-hand version.

The **Vulcan RFID™ PAR90209H** is an ideal antenna for the following applications:

- Warehousing
- Distribution Centers
- Airports and Hospitals
- Transit Terminals
- Conveyor Belts

PRODUCT SPEC SHEET

VULCAN RFID

## Specifications

| | | |
|---|---|---|
| ELECTRICAL | Operating Frequency: | FCC (902-928 Mhz) |
| | Polarization: | Right hand circular |
| | Gain: | 9.0 dBic |
| | Max Read Distance: | Testing recommended |
| | Elevation Beamwidth: | 70° |
| | Azimuth Beamwidth: | 70° |
| | VSWR: | 1.3:1 |
| | Front to Back Ratio: | 20 dB |
| | Axial Ratio: | 1 dB typical |
| | Nominal Impedance: | 50 Ω |
| | Anti-Static Protection: | DC grounded |
| | Antenna Detection: | Not Published |
| | Maximum Input Power: | 10 W |
| MECHANICAL | Connector Type: | N-Type female (connects to N-Type male) |
| | Mounting: | Threaded stud |
| | Cable: | Not included |
| | Dimensions: | 259 x 259 x 33.5 mm (10.2 x 10.2 x 1.32 in) |
| | Weight: | 1 kg (2.3 lbs) |
| | Radome Material: | High Strength PC |
| ENVIRONMENT | Operating Temperature: | -25°C to +70°C (-13° to +158°F) |
| | IP Rating: | IP 67 |
| | | |
| | | |
| | | |
| | | |

# APPENDIX C: Impinj RFID Reader Datasheet

| Product Details | Speedway R420 | Speedway R220 | Speedway R120 |
|---|---|---|---|
| Use Cases | Optimized for 4 read zone use cases<br>Expandable to 32 read zones with Impinj Antenna Hubs<br>Up to 1,100 tag reads per second | Optimized for 2 read zone use cases<br>Up to 200 tag reads per second | Optimized for 1 read zone use cases<br>Expandable to 8 read zones with optional Impinj Port Pack<br>Up to 200 tag reads per second |
| Antenna Ports | 4 | 2 | 1 |
| Read Zones (maximum) | 32 with Antenna Hubs | 2 | 8 with Port Pack |
| Transmit Power (maximum without Antenna Hub) | FCC: 32.5 dBm AC/ 31.5 dBm PoE<br>ETSI: 31.5 dBm AC/ 30.0 dBm PoE | FCC: 32.5 dBm AC/ 31.5 dBm PoE<br>ETSI: 31.5 dBm AC/ 30.0 dBm PoE | FCC: 30.0 dBm AC and PoE<br>ETSI: 30.0 dBm AC and PoE |
| Air Interface Protocol | GS1/EPCglobal UHF Gen2 (ISO 18000-63) or RAIN RFID | | |
| Receive Sensitivity (maximum) | - 84dBm | | |
| Return Loss (minimum) | 10dB | | |
| Reliability | Enterprise Grade | | |
| Network Connectivity | 10/100BASE-T Ethernet | | |
| GPIO Support | Yes | | |
| USB Ports | 1 device (Type B), 1 host (Type A) | | |
| Management Console Port | RS-232 using a standard Cisco-style management cable (DB-9 to RJ-45) | | |
| Power Sources | 802.3af PoE or AC-DC power supply rated for 24Vdc/2.1A | | |
| Environmental Sealing | IEC IP52 | | |
| Shock and Vibration | MIL-STD-810G | | |
| Operating Temperature | -4°F to 122°F (-20°C to 50°C) | | |
| Humidity | 5% to 95% non-condensing | | |
| Dimensions (H x W x D) | 7.5 x 6.9 x 1.2 in (19 x 17.5 x 3 cm) | | |
| Weight | 1.5 lb (.7 kg) | | |
| RF Certifications | www.impinj.com/supported_regions | | |
| RoHS Compliant | Yes | | |
| Speedway SDK, ETK and LTK library support | Yes | | |
| Warranty and Maintenance Options | 1 year limited warranty with purchase, option to extend 3 year Enhanced Maintenance upgrade available | | |

**APPENDIX D: Python Code**

```
from time import strptime

import pandas as pd

import datetime as dt

import numpy as np

from datetime import datetime

import time



timestamp1 = tag_data['// Timestamp']     # Counting total seconds in different feature

seconds=[]

for i in timestamp1:

  seconds.append(time.mktime(i.timetuple()))    # Shows the total seconds until recorded time

tag_data['Seconds']=seconds

tag_data.head()

act_cor = np.array([[0,0,0], [45,0,0], [90,0,0], [135,0,0], [0,0,36],
```

```
        [45,0,36], [90,0,36], [135,0,36], [0,0,72], [45,0,72],

        [90,0,72], [135,0,72], [0,0,108], [45,0,108], [90,0,108],

        [135,0,108], [0,45,0], [45,45,0], [90,45,0], [135,45,0],

        [135,90,0], [90,90,0], [45,90,0], [0,90,0], [0,135,0],

        [45,135,0], [90,135,0], [135,135,0],

        [95,62,66], [88,66,66], [80,59,66], [89,54,66]])
```

```
%%time

EPC_tt = split_data['EPC_TT']

EPC_rt = split_data['EPC_RT']



X_tt=[]

Y_tt=[]

Z_tt=[]

X_rt=[]
```

```
Y_rt=[]

Z_rt=[]


for i in range(len(EPC_tt)):                # Iterate through each of the rows in after_split_data and
get cordinates X,Y,Z from act_cor dataframe

  X_tt.append(act_cor.loc[EPC_tt[i], 'X'])

  Y_tt.append(act_cor.loc[EPC_tt[i], 'Y'])

  Z_tt.append(act_cor.loc[EPC_tt[i], 'Z'])

  X_rt.append(act_cor.loc[EPC_rt[i], 'X'])

  Y_rt.append(act_cor.loc[EPC_rt[i], 'Y'])

  Z_rt.append(act_cor.loc[EPC_rt[i], 'Z'])
```

```
%%time

from sklearn.model_selection import train_test_split

X_train, X_test, y_train, y_test = train_test_split(X,y,test_size=1/5,shuffle=False) # 20% test
data without shuffling
```

```python
from xgboost import XGBClassifier

xgb = XGBClassifier()

xgb.fit(X_train, y_train)
```

```python
from sklearn.preprocessing import StandardScaler

z_after_split_data = StandardScaler().fit_transform(split_data.drop(['// Timestamp_x','// Timestamp_y'],axis=1))

z_after_split_data

# Don't need to scale our target, and will be cumbersome to select X from z_after_split_data

z_fit = StandardScaler().fit(X_train)

z_X_train = z_fit.transform(X_train)

z_X_test = z_fit.transform(X_test)

z_X_test
```